IOPscience iopscience.iop.org

Home Search Collections Journals About Contact us My IOPscience

Adsorbate reactivity and thermal mobility from simple modeling of high-resolution core-level spectra: application to O/Al(111)

This article has been downloaded from IOPscience. Please scroll down to see the full text article.

2009 J. Phys.: Condens. Matter 21 265003

(http://iopscience.iop.org/0953-8984/21/26/265003)

View the table of contents for this issue, or go to the journal homepage for more

Download details:
IP Address: 129.252.86.83
The article was downloaded on 29/05/2010 at 20:18

Please note that terms and conditions apply.

J. Phys.: Condens. Matter **21** (2009) 265003 (7pp) doi:10.1088/0953-8984/21/26/265003

Adsorbate reactivity and thermal mobility from simple modeling of high-resolution core-level spectra: application to O/Al(111)

Jakob Schouborg, Merete K Raarup[1] and Peter Balling

Department of Physics and Astronomy, University of Aarhus, DK-8000 Aarhus C, Denmark

E-mail: balling@phys.au.dk

Received 29 January 2009, in final form 30 April 2009
Published 27 May 2009
Online at stacks.iop.org/JPhysCM/21/265003

Abstract

A high-resolution core-level spectroscopy investigation of the adsorption of oxygen on Al(111) at variable oxygen exposure demonstrates a low surface reactivity for an intensively cleaned surface. The threshold for oxide formation is as high as ∼200 L (langmuirs), at which point the coverage of the chemisorbed oxygen exceeds half a monolayer. A simple model is presented, using which it is possible to deduce the oxygen coverage from the core-level spectra and determine the initial sticking probability. For our data a value of 0.018 ± 0.004 is obtained. The changes in core-level spectra following low-temperature annealing of low-coverage O/Al(111) reflect the formation of gradually larger islands of oxygen atoms (Ostwald ripening). The island formation is consistent with a random-walk model from which the diffusion barrier can be deduced to be in the range of 0.80–0.90 eV.

1. Introduction

The oxidation of aluminum has been studied extensively by many groups using a wealth of different techniques (for a recent review, see [1, 2]). It is generally accepted that adsorption of O_2 on Al(111) initially leads to the formation of a dissociative chemisorbed phase with the oxygen atoms residing in fcc type three-fold hollow sites. Scanning tunneling microscopy (STM) studies have indicated that at increased coverage, small (1×1) islands are formed and that long before saturation occurs, oxide formation sets in [3]. The most recent results point towards an adsorption mechanism which is a combination of ordinary chemisorption and abstractive adsorption with the latter dominating at low incident energies [2, 4].

The structural assignment of the chemisorbed phase discussed above is supported by core-level spectroscopy data which have shown the existence of three chemisorption-related peaks and one oxide peak adjacent to the Al 2p peaks on the high-binding-energy side [5–7]. The Al 2p peaks on the Al(111) surface exhibit surface core-level shifts smaller than 15 meV [5]. The three sub-oxide peaks were found to be shifted by 0.49, 0.97 and 1.46 eV with respect to the Al $2p_{3/2}$ level at 72.7 eV while the broad oxide peak was shifted by 2.5–2.7 eV [5] (see also figure 1). The three sub-oxide peaks were observed to show up sequentially, following an increase in oxygen coverage, with the 0.49 eV peak appearing first. The latter was hidden by the $2p_{1/2}$ peak at 73.1 eV while the other peaks were clearly visible. The three sub-oxide peaks have been associated with Al atoms binding to one, two and three oxygen atoms, respectively, as can be rationalized from a simple electrostatic picture of core-level spectroscopy, with the oxygen atoms representing an electro-negative environment. This corresponds to Al atoms situated at the edges and in the interior of an oxygen island where the coordination numbers to oxygen atoms are one (or two) and three, respectively [3], see also figure 2(b). In a single high-resolution (50 meV) study, an additional shoulder on the low-binding-energy side of the Al 2p peaks was observed and ascribed to atoms sitting in a metallic environment, most likely in a (mono-atomic) semi-amorphous Al layer situated at the Al–Al_2O_3 interface [6].

[1] Present address: Stereology and Electron Microscopy Research Laboratory, University of Aarhus, DK-8000 Aarhus C, Denmark.

 © 2009 IOP Publishing Ltd Printed in the UK

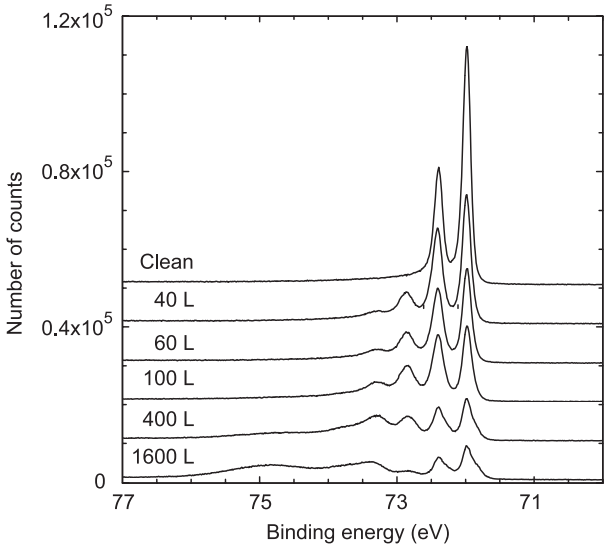

Figure 1. Measured core-level spectra with different oxygen doses as indicated in the figure.

The adsorption of oxygen molecules on the Al(111) surface is characterized by an unusually low initial sticking probability (see [1] and references herein). Recent theoretical developments have explained this low sticking probability, which is strongly at variance with adiabatic models, by spin selection rules that give rise to nonadiabatic behavior [1, 8]. An investigation by Yates *et al*, using high-resolution electron-energy-loss spectroscopy (HREELS), has indicated that the apparent disagreement in previous measurements of the reactivity may have been due to different defect densities of the chemically clean Al(111) surfaces used by different groups as discussed in [9]. The investigation showed that it was only possible to obtain reproducible oxygen uptake curves after extreme levels of cleaning (sputter/anneal cycles with several tens of hours of sputtering).

In the present paper the results of a high-resolution core-level spectroscopy investigation of the O/Al(111) system are reported. The oxygen uptake is investigated for a well-prepared aluminum surface and a model for the extraction of coverages from the core-level spectra is described. The properties of the surface are further investigated by studying the response of the low-oxygen-coverage surface to moderate annealing allowing us to obtain an estimate of the diffusion barrier.

2. Experimental setup

The experiments were performed at the SGM-I synchrotron-radiation beam line at the ASTRID storage ring at the University of Aarhus, Denmark. The SGM-I beam line has a spherical-grating monochromator, which can be operated in the 25–300 eV photon-energy range. For the present experiment, a photon energy of 130 eV with a resolution of 50 meV (FWHM) was used. At the end of the beam line an ultra-high-vacuum (UHV) analyzing chamber is installed and the sample can be moved to a preparation chamber equipped with standard UHV surface science diagnostics. The synchrotron-radiation beam

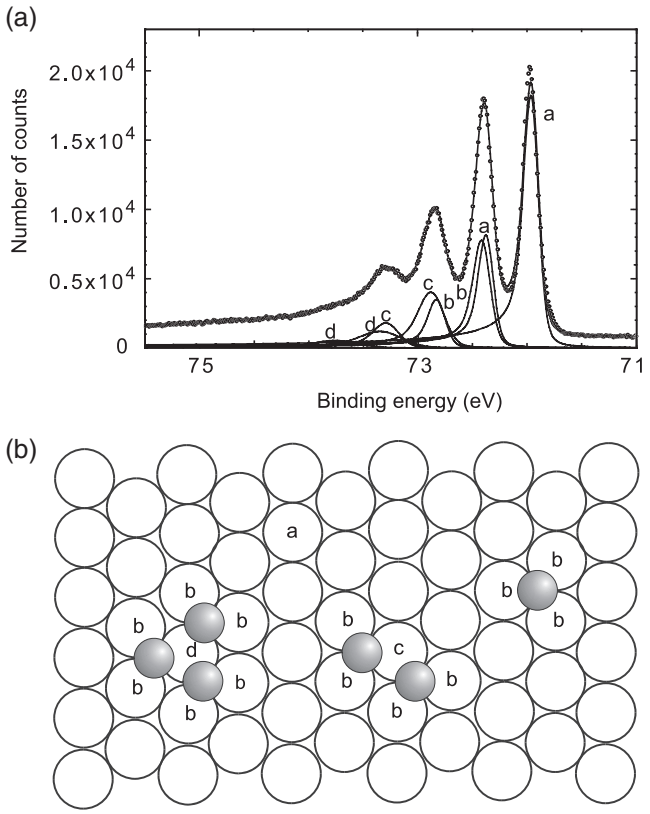

Figure 2. (a) An example of the fit of an Al 2p core-level spectrum at 100 L dosage to the four components corresponding to clean aluminum (labeled a) and Al atoms near 1, 2, and 3 oxygen atoms, labeled b, c, and d, respectively. (b) A sketch of the Al(111) surface with the three smallest island sizes indicated and the surrounding Al atoms marked by the appropriate label.

is incident on the surface at 35° with respect to the surface normal and photoelectrons within a ∼0.1 steradian space angle normal to the surface are collected with a SCIENTA electron spectrometer [10]. The electrons are focused onto the entrance slit of the spectrometer by a lens system and are dispersed according to their kinetic energy by the radial electrostatic field between two hemispheres. Due to the spherical symmetry of the spectrometer, the entrance slit is imaged onto the detection system consisting of a multi-channel-plate detector and a charge-coupled-device camera. In the experiment the spectrometer was operated with a resolution of 70 meV.

The Al(111) surface was cleaned with Ar^+ sputtering (1 keV, 3 μA) and subsequent annealing to 400 °C, see details below. The sample was cooled during measurements (−80 °C) with a liquid nitrogen purge to minimize phonon broadening of the core-level spectra. The temperature was measured using an N-type thermo-couple attached to the rear side of the sample. The measurements were performed at a base pressure of $\sim 5 \times 10^{-10}$ Torr in the analyzing chamber.

Adsorption of oxygen was performed at low temperature (−80 °C) by exposing the Al(111) crystal to pure oxygen (99.998%) at a pressure of approximately 10^{-7} Torr in the preparation chamber. To obtain the desired oxygen dosage the sample was exposed to O_2 for an appropriate period of time (1 L = 10^{-6} Torr s). For a sequence of spectra acquired with an

increasing oxygen coverage (section 3), an additional amount of O_2 was added to the existing oxygen layer on the Al surface.

3. Evaluation of the oxygen uptake

According to the HREELS study by Yates *et al* an extensive sputtering time (up to 56 h) is needed to obtain an Al surface with a small number of defect sites [9, 11]. In figure 1 the core-level spectra recorded after an extensive sputter/anneal treatment of the Al surface are shown. The sample was sputtered for a total of 45 h and 40 min and annealed at 400 °C for 110 min. This was done by four cycles of sputtering (∼12 h) followed by annealing (∼1/2 h). Together with the spectrum of the clean Al(111) surface, spectra corresponding to an exposure of 40, 60, 100, 400 and 1600 L of oxygen are shown. The evolution of the various sub-oxide peak components is clearly visible simultaneously with a decrease in the original Al peaks. Core-level spectra similar to the ones shown in figure 1 were recorded before the long-time sputtering. In these spectra (not shown) one finds that the growth of the oxygen-induced peaks develop significantly faster with dosage.

Fitting the spectra using a Doniach–Sunjic line shape convoluted with a Gaussian function [12] gave a quantitative way of comparing the two sets of spectra. A fit of the 100 L spectrum is shown in figure 2(a). The labels a, b, c, and d refer to clean Al, and Al binding to one, two and three oxygen atoms respectively, as illustrated in figure 2(b) for various oxygen islands. In figure 3 the intensities of the various peak components (normalized to the intensity of the clean spectrum) are plotted as a function of oxygen exposure.

One can see that the oxide peak in the spectra acquired before the long-time sputtering, figure 3(a), contributes by a relative intensity of more than 5% already in the 60–100 L range, while a similar intensity is not seen until ∼200 L in the long-time-sputtered spectra, figure 3(b). At high coverages, the intensity of the b-peak (Al binding to one oxygen atom) is seen to decrease in both cases, but the decrease is significantly slower in the long-time sputtered case, figure 3(b). A similar tendency is seen for the c-peak. The d-peak is growing together with the oxide peak as a function of increased O_2 dosing in the first spectra, figure 3(a), but in figure 3(b) there is clearly a range of dosage where only the chemisorbed features are seen *before* the oxide formation sets in. This is consistent with the observation in [3] that oxide nucleation originates at steps and supports our interpretation of the long-time sputtered surface as having a smaller abundance of steps and defects.

The overall trends in figure 3 are in agreement with earlier core-level spectroscopy results [5] which postulated that the peaks which here are labeled b, c, and d should appear one after the other, starting with peak b.

3.1. Simple model for extraction of adatom coverages

Approximate values for the relative distribution of single isolated oxygen atoms, two-atom oxygen islands (in the following referred to as dimers) and three-atom oxygen islands (trimers) as a function of oxygen coverage can be derived

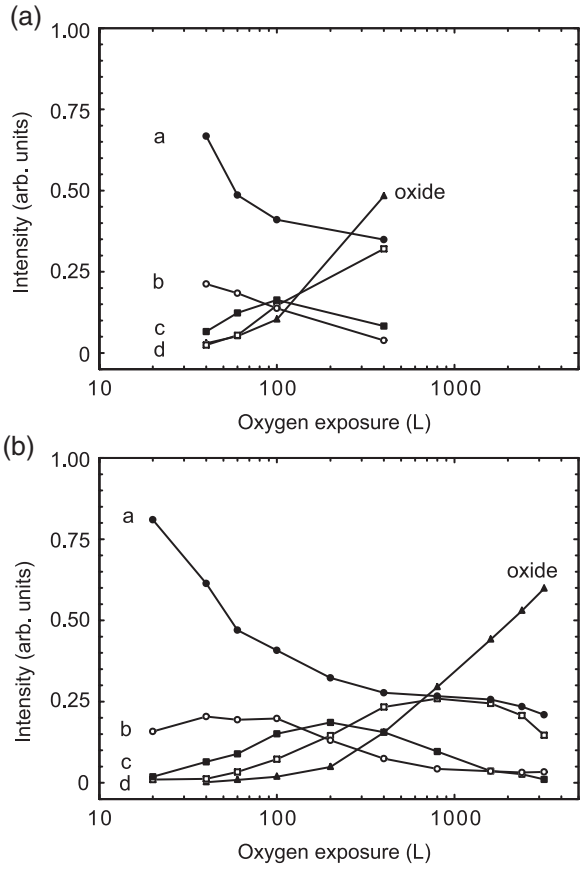

Figure 3. Intensity of the various peaks from the Al 2p core-level spectra versus oxygen dosage. (a) Data taken before the long-time sputtering, (b) the evolution after the extended cleaning cycles. The signal from clean Al, a-type, is represented by ●, signal from Al bonding to one oxygen atom, b-type, by ○, Al bonding to two oxygen atoms, c-type, by ■, and Al bonding to three oxygen atoms, d-type, by □. The signal from oxide is indicated by ▲. The lines are drawn to guide the eye.

from the spectra using relatively simple geometric arguments. As shown in figure 2(b), a single isolated oxygen atom is associated with three b-peak-type Al atoms, an oxygen dimer produces four b-type Al atoms and one c-type Al atom. Finally, oxygen trimers give rise to six b-type Al atoms and one d-type Al atom. Note that this argument requires that nearest-neighbor effects play the dominant role, i.e. that for instance a 'b'-type atom at a monomer site is indistinguishable from a 'b'-type atom at a trimer. Since the mobility of the oxygen atoms is vanishingly small for the cooled surface (see section 4), it will be reasonable to assume a small frequency of larger islands at low coverage. Other configurations with three (or even four) oxygen adatoms are in principle possible, but these will have low frequency and thus play a minor role. Theoretical calculations [13] show that the closed islands are energetically most favorable, e.g. the difference in binding energy between a closed trimer and a trimer aligned along one crystallographic direction is 0.07 eV/oxygen atom. Based on this, only the closed-island configuration described above was considered in the present model. Under this assumption the spectra can be 'inverted' to provide the distribution of monomers, dimers and

trimers. It is, however, necessary to account for the fact that the photoelectrons from aluminum bound to one, two, and three oxygen atoms on average have penetrated different amounts of oxygen. In the most simple approximation, the electrons from b-type Al atoms go through 1/3 of a monolayer, the electrons from c-type Al atoms penetrate 2/3 of a monolayer and the electrons from d-type Al atoms a full oxygen monolayer. Consequently, in order to obtain the coverage contribution from each type, it is necessary to normalize the measured relative intensity (i.e. relative to the area of the 'clean' peak at zero coverage) to the effective transmission, $(2/3+1/3T_O)$ (b-type), $(1/3+2/3T_O)$ (c-type), and (T_O) (d-type), where T_O is the transmission coefficient of the complete oxygen monolayer.

Before developing this model further, a few comments on the mechanisms that are neglected in this simple transmission-coefficient approach are given. One mechanism that can be important in core-level experiments is photoelectron diffraction. In the present experiment, with kinetic energies of roughly 50 eV, the de Broglie wavelength (1.73 Å) becomes comparable to the Al nearest-neighbor distance, $a_s = 2.86$ Å. Although this means that diffraction effects can potentially be very strong, this effect is not included in the model. This is partly motivated by the fact that the solid angle from which the photoelectrons are collected is quite large; the 0.1 steradian space angle corresponds to a cone with a $\sim 20°$ opening angle, and since all spectra are recorded by collecting electrons emitted normal to the surface, diffraction effects are to some degree averaged out. The use of the same photon energy and emission angle in all the recorded spectra minimizes the diffraction effects. Finally, the recorded photoelectron peak amplitudes exhibit a smooth dependence on the coverage, e.g. the attenuation of the signal from the clean (a-type) Al atoms, cf figure 3. This indicates that diffraction issues play a minor role and may justifiably be neglected. With these precautions in mind, the simple model is described.

The transmission coefficient of the oxygen monolayer needed for the island-distribution estimates can be found from the data by analysis of the development of the different peaks with coverage. The development of the curves in figure 3(b) can be interpreted as the formation of an almost full monolayer of chemisorbed oxygen, before oxide formation really sets in: the 'clean' Al peak (labeled a) is attenuated and the chemisorbed species are gradually transformed into larger and larger islands, causing b-, c- and d-type Al atoms. The original signal (at zero dose) in the a peak consists of both a surface, I_a^S, and a bulk component, I_a^B, where the bulk component is attenuated by T_{Al} due to transmission through the surface aluminum layer. We thus have $I_a(0) = I_a^S + T_{Al} I_a^B$. As the coverage approaches one monolayer, all the intensity of the surface atoms is converted into signal from the b-, c- and d-type Al atoms. One then obtains $T_O I_a^S = I_b(\infty) + I_c(\infty) + I_d(\infty)$, where T_O is the transmission of an oxygen monolayer and I_b, I_c and I_d represent the signal from the b-, c- and d-type Al atoms. The argument '∞' is used to denote the limiting value of intensities just before oxide formation sets in. The sum from the experimental data does converge (around 400 L) to $I_b(\infty) + I_c(\infty) + I_d(\infty) = 0.46$ (relative to $I_a(0)$, the clean peak at zero coverage), and this value is assumed to correspond to 1 ML of coverage.

The residual signal in the a-peak at higher coverage is due to the bulk component. In the same approximative description of transmission, the bulk component I_a^B will then give rise to an intensity $I_a(\infty) = T_O T_{Al} I_a^B$. The signal I_a of the a peak levels off at $I_a(\infty) = 0.26$. It can be seen that

$$I_a(\infty) + I_b(\infty) + I_c(\infty) + I_d(\infty) = T_O T_{Al} I_a^B + T_O I_a^S = T_O(T_{Al} I_a^B + I_a^S) = T_O I_a(0). \quad (1)$$

This equation expresses that upon completion of an oxygen monolayer, the original signal from the clean surface, $I_a(0)$, is attenuated by T_O. The oxygen transmission coefficient can then be estimated to $T_O = 0.72$. Knowing T_O the intensity of the surface component can be found: $I_a^S = 0.46/T_O = 0.64$. This gives the values needed for the following calculations.

The extraction of an island size distribution can only be obtained at the absence of larger islands. Let us consider the minimum dose used, 20 L, for the long-time sputtered surface. The data at this low coverage did not show any sign of the d-type aluminum, and a fit to the other three components gave relative intensities (i.e. normalized to $I_a(0)$) of 15% for the b peak and 1.9% for the c peak. When remembering that in the island configurations considered here, only one c-type aluminum arises from a dimer configuration and when correcting for the approximate transmission coefficient calculated above, a value of $\theta_2 = 0.036$ ML for the density of islands with dimers is obtained. To find the number of isolated oxygen atoms, it must be considered that 4 atoms in the b peak are required for each Al atom in the c peak (figure 2(b)). Since each isolated oxygen atom gives signal from three b-type atoms, a density of $\theta_1 = \frac{1}{3}[I_b(20\text{ L})/(I_a^S(2/3 + 1/3T_O)) - 4\theta_2] = 0.036$ ML of truly isolated oxygen atoms is found. On the basis of the island distribution, the overall coverage can easily be calculated as $\theta = \theta_1 + 2\theta_2$. Using the values of the oxygen transmission coefficient and surface component intensity gives a coverage of $\theta = 0.11$ ML.

The resulting densities of $\theta_1 = 0.036$ ML and $\theta_2 = 0.036$ ML ($-80\,°$C) for the long-time sputtered surface correspond to 50% of the islands consisting of single atoms and 50% consisting of dimers. Since the interaction between adsorbed oxygen atoms is attractive [3], the observed frequency of isolated atoms is a lower limit. It can therefore safely be claimed that more than one third of the oxygen molecules adsorb with an atom separation exceeding the Al nearest-neighbor spacing, a_s.

To determine whether the observed distribution reflects a clustering of atoms due to the adsorption process, it is useful to estimate the probability of 'coincidental' pairs. Each aluminum atom has three possible fcc-binding sites surrounding it, see figure 2(b), and each of these sites are occupied with probability θ. The probability to become an a-, b-, c- or d-type aluminum atom can then be found using a binomial distribution. With $\theta = 0.11$ ML a distribution of 0.70, 0.27, 0.035, and 0.0015 for the four aluminum types is found. Using the same inversion methods as described above, it can be seen that this random distribution of oxygen corresponds to $\tilde{\theta}_1 = 0.040$ ML, $\tilde{\theta}_2 = 0.035$ ML and $\tilde{\theta}_3 = 0.0015$ ML. This shows that, at the coverages applied in the present investigation, the ratio of single isolated oxygen atoms

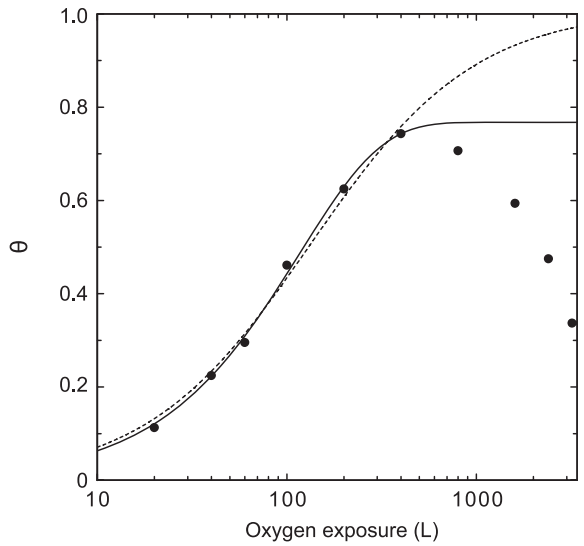

Figure 4. The coverage as a function of dosing (●) derived from the core-level spectra through equation (2). The two lines represent fits to the measured points according to Langmuir theory of a first-order (solid line) and second-order (dashed line) adsorption process. The apparent disagreement above 400 L is due to oxide formation, see description in the text.

to oxygen pairs is consistent with a random distribution of atoms on the surface. It is thus not possible by means of high-resolution core-level spectroscopy to distinguish between the different adsorption mechanisms proposed on the basis of other experimental approaches, since the changes in the core-level spectra below a 20 L dose are too small for reliable analysis.

At larger coverages, it is no longer feasible to derive the density of the different island sizes. The oxygen coverage can, however, still be derived from the core-level spectra, since independently of the geometric configuration, the coverage can be expressed as

$$\theta = \frac{1/3I_{\mathrm{b}}}{I_{\mathrm{a}}^{\mathrm{S}}(2/3 + 1/3T_{\mathrm{O}})} + \frac{2/3I_{\mathrm{c}}}{I_{\mathrm{a}}^{\mathrm{S}}(1/3 + 2/3T_{\mathrm{O}})} + \frac{I_{\mathrm{d}}}{I_{\mathrm{a}}^{\mathrm{S}}T_{\mathrm{O}}}, \quad (2)$$

which still assumes the simple description of transmission outlined above. The oxygen coverage versus dosage calculated from this expression is plotted in figure 4.

3.2. Determination of the initial sticking probability

The average sticking probability for coverages between 0–0.11 ML (20 L) can be calculated as 0.018 ± 0.002 [14], where the uncertainty represents a statistical spread of one standard deviation for the line shape fitting parameters. By in addition incorporating an estimated uncertainty of 10% on the pressure measurement, a result of 0.018 ± 0.004 is obtained. This sticking coefficient is in agreement with the most recent experimental investigations. In [9] temperature-dependent sticking coefficients measured at 48 and 30 L are reported. The sticking coefficient at a temperature similar to the −80 °C used in the present study is 0.016, in very good agreement with our results. In [15] the sticking coefficient as a function of the incident translational energy of a molecular beam is measured at low oxygen coverages. At energies corresponding to thermal energies (24 meV), a sticking coefficient of 0.015 ± 0.005 is reported with no significant temperature dependence. The present sticking probability is in excellent agreement with the recent theoretical estimates including nonadiabaticity originating from spin selection rules [1, 8].

An alternative method to obtaining the initial sticking probability is based on Langmuir adsorption theory, which provides an expression for the adsorption rate [14]

$$N_0 \frac{\mathrm{d}\theta}{\mathrm{d}t} = s_0(1-\theta)^n \frac{P}{\sqrt{2\pi mkT}}, \quad (3)$$

where s_0 is the initial sticking probability, N_0 is the surface density of Al(111), m is the molar mass of oxygen, P and T the partial pressure and temperature of the oxygen gas, and n is the adsorption order. The first-order process, $n = 1$, is abstractive adsorption where only one of the oxygen atoms is adsorbed on the surface and the other ejected back to the gas phase, cf e.g. [16]. Using equation (3) the adsorption rate becomes

$$\theta = 1 - \exp(-Cx), \quad (4)$$

where x is the exposure (proportional to the dose in langmuirs) and C is a constant containing the initial sticking probability s_0. For a second-order adsorption process ($n = 2$, dissociative adsorption) equation (3) gives an adsorption rate of

$$\theta = 1 - \frac{1}{Cx + 1}. \quad (5)$$

In figure 4 the fit of equations (4) and (5) to the coverage found by equation (2) is shown for the low coverages. The overall agreement is fairly good over the range applied for the fit, up to a dose of 400 L.

Both the first- and the second-order curves fit the data points qualitatively. However, the present data do not allow a distinction between the firsts- and second-order process. The trend in the data seems to be in slightly better agreement with the first-order model, but the model fails to predict convergence to 1 ML, which is not the case with the second-order model. The fitting yields values of C from which the initial sticking coefficient can be found. By assuming a first-order process a value of $s_0 = 0.020 \pm 0.006$ is obtained, whereas the second-order process gives $s_0 = 0.020 \pm 0.007$. These values of the initial sticking coefficient were found using data points at low coverage in the fits, up to 100 L. By including more high-dosage data points in the fits the apparent sticking coefficients increase, indicating that Langmuir adsorption theory only gives a good description at low coverages. At the higher dosages the adsorption processes will presumably be influenced by the inter-adsorbate attraction [17], making the Langmuir theory inapplicable. The apparent disagreement between the data points and the fits above 400 L presumably is due to oxide formation which removes intensity from the chemisorbed species. The values of the initial sticking coefficient found from the fitting of the coverage versus dose are in excellent agreement with the value obtained from the coverage at 20 L described above.

The coverage at the point where oxide formation sets in can be estimated by comparison of figures 3 and 4. It is

seen that this happens at ∼200 L where $\theta \approx 60\%$, which is significantly higher than in most previous observations. Reference [3] reports oxide formation at a 60 L dose of O_2 corresponding to a coverage of 20%, whereas [6, 7] do not give the coverages, but report oxide formation at dosages in the range 40–60 L. As discussed by Zhukov *et al* [9], many previous investigations reported initial oxide formation in the 50–70 L range, while their study on the well-prepared surface showed no oxide formation below an exposure of ∼200 L [11] in good agreement with the present study. Most likely, the different observations are an effect of variations in the surface quality, as discussed above. Other sources of error are the absolute calibration of the applied dose (pressure gauges and inlet geometry).

4. Annealing of O/Al(111): determining the diffusion barrier

In another series of measurements, high-resolution core-level spectra were recorded after annealing of the sample to different temperatures. These experiments provide information about the mobility of the adsorbed oxygen atoms. STM studies by Trost *et al* [18] have shown that for temperatures above 300 K (23 °C), the otherwise immobile oxygen adatoms become mobile and start to form larger oxygen islands on the Al surface. An x-ray photoelectron spectroscopy (XPS) experiment by Zhukov *et al* [9] showed that the surface sticking probability was temperature dependent, and they were able to distinguish between the signal from chemisorbed oxygen and from oxide. By annealing from 243 K (−30 °C) up to 773 K (500 °C) they found that all the chemisorbed oxygen transformed into oxidic oxygen.

In the present experiment, the extensively cleaned Al(111) surface was dosed with different amounts of oxygen as described in section 2. At each oxygen dose a spectrum was acquired at low temperature (−80 °C) as well as after the sample had been annealed subsequently at 20, 50 and 100 °C for 10 min each. Between the measurements for the different oxygen doses, the sample was cleaned by sputtering and annealing to get a chemically clean surface as indicated by the absence of oxygen-induced features in the core-level spectra. The temperature investigations were performed with oxygen coverages of 20, 40 and 100 L. The produced spectra were analyzed as described above (cf section 3).

The measured intensities of the a, b, c, and d peaks versus the annealing temperature for a dosage of 20 L is shown in figure 5. The signals from peaks a and c stay fairly constant as the temperature is increased. The intensity of the b peak is seen to decrease with increasing temperature. The d peak behaves with the opposite trend, the signal increasing with temperature. The results for Al(111) covered with 40 and 100 L of oxygen (not shown) look similar to the results shown in figure 5, with the modification that the b, c and d signals naturally reflect the higher doses of oxygen. In no cases was oxide formation observed within the temperature range investigated here. This is consistent with the XPS experiment by Zhukov *et al* [9]. Previous core-level investigations reported oxide formation at room temperature (300 K) in the same range of coverages as investigated here [7, 6]. In STM studies, oxide formation was reported at room temperature (300 K) with a coverage of 60 L [3], or at low coverage (3 L) at higher temperatures, 440 K (167 °C), just above the temperatures used here [18].

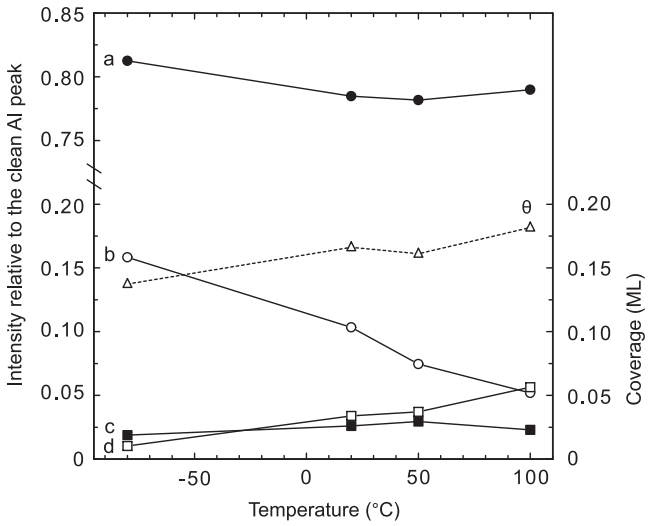

Figure 5. Amplitude of the clean Al peak and the three chemisorbed features versus annealing temperature for a coverage of 20 L on the Al(111) surface. Note the broken scale on the left y-axis. The signal from clean Al, a-type, is represented by ●, signal from Al bonding to one oxygen atom, b-type, by ○, Al bonding to two oxygen atoms, c-type, by ■, and Al bonding to three oxygen atoms, d-type, by □. The △ shows the oxygen coverage, θ. The lines are drawn to guide the eye.

Figure 5 also shows the coverage calculated from the signal intensities in the simple transmission model, equation (2). Within the range of precision (∼10%) the coverage is almost constant as a function of the annealing temperature. The slightly increasing tendency might be an indication that our simple model for the transmission is not complete and that the error introduced by the model has a weak dependence on the island distribution. The fact that the coverage is approximately independent of the annealing temperature shows that, as expected, there is no thermal desorption in the range of temperatures studied here. It is also consistent with the absence of oxide formation, since oxide formation would lead to a loss in the coverage found from the three chemisorbed species.

The behavior seen in figure 5 is well explained by the aggregation of oxygen atoms on the Al surface. When the temperature becomes high enough to allow a finite mobility of oxygen, the oxygen atoms migrate on the surface and, due to the attractive potential between adatoms, form gradually larger islands (Ostwald ripening). The formation of oxygen dimers or trimers leads to a decrease in the b-peak intensity. The c-peak intensity reflects the number of dimers and since it is staying fairly constant initially, it must reflect an approximate balance between the creation of dimers from single atoms and the loss of dimers to larger islands. Eventually larger islands start to dominate and the d peak becomes prevailing.

Using a random-walk approach as in Chakarova *et al* [19], one can find the number of 'hops' which the oxygen atoms

perform at a given temperature during the time of annealing. Assuming that an atom only jumps to its neighboring site, the number of 'hops' necessary to enable an oxygen atom to meet a neighbor at a given coverage can be estimated by considering a random walk on the Al(111) surface. It is assumed that the atoms perform a random walk with a given probability per time until they meet another oxygen atom. The motion of oxygen pairs is highly improbable, since the barrier for this collective diffusion is much higher. On the other hand, formed pairs of atoms could in principle dissociate again, but theoretical estimates suggest a binding energy of 0.21 eV [13], which would significantly increase the barrier for diffusion out of a pair. This breakup of pairs (and larger islands) is neglected in the present model. At the minimum coverage used here, $\theta = 0.11$ ML at 20 L dosage, the average separation between a random distribution of oxygen atoms is $\sim 3a_s$, where a_s is the Al nearest-neighbor spacing. This means that in order to explain the aggregation deduced from figure 5, the random walk must cover approximately this distance. On the other hand, if the distance traveled is very long already after 10 min at the lowest temperature investigated, 20 °C, all the changes would have occurred in this first spectrum. In other words, the fact that aggregation happens within the temperature interval considered here, puts fairly strict bonds on the activation barrier for surface diffusion. Examining the hopping rate with different diffusion barriers assuming a pre-factor of 10^{-13} s^{-1} and comparing to the oxygen nearest-neighbor distance at the coverages considered, shows that the aggregation observed in this experiment is consistent with a diffusion activation barrier in the range 0.80–0.90 eV. For instance, a diffusion barrier of 0.85 eV gives random-walk lengths of $3.8a_s$, $18a_s$, and $140a_s$ during 10 min at the three temperatures applied, which will explain the observed behavior. On the other hand, at diffusion barriers of 0.80 and 0.90 eV, the random walk at 20 °C becomes too long ($10a_s$) and too short ($0.1a_s$), respectively, to explain the observed changes in the spectrum.

This result is lower than the value of 1.0–1.1 eV deduced from the experimental STM data [3, 18], but slightly higher than the values of 0.7–0.8 eV obtained from theoretical calculations [17, 20]. In any case, it is clear from the changes occurring already in the room-temperature spectrum that the adsorbed oxygen is by no means immobile at room temperature for up to 1 h [21], and for a 120 s time interval [3], as was claimed by STM studies. In these studies the oxygen was, however, dosed at room temperature, while the present investigation applied dosing at −80 °C. It cannot be excluded that the adsorption temperature influences the binding of the adsorbed oxygen atoms.

5. Summary

High-resolution core-level spectroscopy has been used to investigate the adsorption process of O_2 on Al(111). After an extended cleaning cycle the surface reactivity was low, and it was possible to complete more than half a monolayer of chemisorbed oxygen, before oxide formation set in. A simple model was developed by which the initial sticking probability could be calculated from core-level spectra acquired as a function of oxygen exposure. The sticking probability obtained this way agrees well with recent experimental findings. Annealing investigations showed that the chemisorbed phase was stable towards oxide formation up to 100 °C for 10 min. Instead the annealing gave rise to an aggregation of the islands to larger and larger sizes starting already at room temperature. Based on a random-walk model, an activation barrier of 0.8–0.9 eV for surface diffusion of single oxygen atoms was obtained.

Acknowledgments

We wish to acknowledge J H Pedersen for his contributions in an early phase of this experiment. We are grateful for the assistance of the entire ISA staff and in particular of Z Li and S V Hoffmann. This work was supported by the Danish Natural Sciences Research Council (SNF).

References

[1] Behler J, Reuter K and Scheffler M 2008 *Phys. Rev.* B **77** 115421
[2] Hasselbrink E 2006 *Curr. Opin. Solid State Mater. Sci.* **10** 192
[3] Brune H, Wintterlin J, Trost J and Ertl G 1993 *J. Chem. Phys.* **99** 2128
[4] Andreev E A, Grishin M V, Dalidchik F I, Kovalevskii S A and Shub B R 2005 *Kinet. Catal.* **46** 137
[5] McConville C F, Seymour D L, Woodruff P D and Bao S 1987 *Surf. Sci.* **188** 1
[6] Berg C, Raaen S, Andersen J N, Lundgren E and Nyholm R 1993 *Phys. Rev.* B **47** 13063
[7] Driver S M, Lüdecke J, Dixon R J, Thompson P B J, Scragg G, Woodruff D P and Cowie B C C 1997 *Surf. Sci.* **391** 300
[8] Behler J, Delley B, Lorenz S, Reuter K and Scheffler M 2005 *Phys. Rev. Lett.* **94** 036104
[9] Zhukov V, Popova I and Yates J T Jr 1999 *J. Vac. Sci. Technol.* A **17** 1727
[10] Mårtensson N, Baltzer P, Bruhwiler P A, Forsell J O, Nilsson A, Stenborg A and Wannberg B 1994 *J. Electron Spectrosc. Relat. Phenom.* **70** 117
[11] Zhukov V, Popova I, Formenko V and Yates J T Jr 1999 *Surf. Sci.* **441** 240
[12] Adams D L and Andersen J N (unpublished) The program FitXPS used for the fitting can be found at http://www.sljus.lu.se/download.html
[13] Razaznejad B 2003 From oxygen to oxide: first-principle study of some key aspects *PhD Thesis* Chalmers University of Technology Göteborg, Sweden, see also [20]
[14] Lüth H 1993 *Surfaces and Interfaces of Solids* 2nd edn (Berlin: Springer)
[15] Österlund L, Zorić I and Kasemo B 1997 *Phys. Rev.* B **55** 15452
[16] Komrowski A J, Sexton J Z, Kummel A C, Binetti M, Weiße O and Hasselbrink E 2001 *Phys. Rev. Lett.* **87** 246103
[17] Jacobsen J, Hammer B, Jacobsen K W and Nørskov J K 1995 *Phys. Rev.* B **52** 14954
[18] Trost J, Brune H, Wintterlin J and Ertl G 1998 *J. Chem. Phys.* **108** 1740
[19] Chakarova R, Oner D E, Zorić I and Kasemo B 2001 *Surf. Sci.* **472** 63
[20] Yourdshahyan Y, Razaznejad B and Lundqvist B I 2002 *Phys. Rev.* B **65** 075416
[21] Brune H, Wintterlin J and Ertl G 1992 *Phys. Rev. Lett.* **68** 624